JACC: CARDIOVASCULAR IMAGING VOL. 15, NO. 1, 2022


ORIGINAL RESEARCH

# Clinical Importance of Left Atrial Infiltration in Cardiac Transthyretin Amyloidosis

Francesco Bandera, MD, PhD,[a,b,*] Raffaele Martone, MD,[c,*] Liza Chacko, MD,[d] Sharmananthan Ganesananthan, MS,[d] Janet A. Gilbertson, CSci,[d] Markella Ponticos, PhD,[d] Thirusha Lane, RN, PhD,[d] Ana Martinez-Naharro, MD, PhD,[d] Carol Whelan, MD,[d] Cristina Quarta, MD, PhD,[d] Dorota Rowczenio, PhD,[d] Rishi Patel, MD,[d] Yousuf Razvi, MD,[d] Helen Lachmann, MD,[d] Ashutosh Wechelakar, MD,[d] James Brown, MD,[d] Daniel Knight, MD,[d] James Moon, MD,[e] Aviva Petrie, PhD,[f] Francesco Cappelli, MD,[c] Marco Guazzi, MD, PhD,[a,b] Luciano Potena, MD,[g] Claudio Rapezzi, MD,[h,i] Ornella Leone, MD,[g] Philip N. Hawkins, MD, PhD,[d] Julian D. Gillmore, MD, PhD,[d,*] Marianna Fontana, MD, PhD[d,*]

## ABSTRACT

**OBJECTIVES** The aim of this study was to characterize left atrial (LA) pathology in explanted hearts with transthyretin amyloid cardiomyopathy (ATTR-CM); LA mechanics using echocardiographic speckle-tracking in a large cohort of patients with ATTR-CM; and to study the association with mortality.

**BACKGROUND** The clinical significance of LA involvement in ATTR-CM is of great clinical interest.

**METHODS** Congo red staining and immunohistochemistry was performed to assess the presence, type, and extent of amyloid and associated changes in 5 explanted ATTR-CM atria. Echo speckle tracking was used to assess LA reservoir, conduit, contractile function, and stiffness in 906 patients with ATTR-CM (551 wild-type (wt)-ATTR-CM; 93 T60A-ATTR-CM; 241 V122I-ATTR-CM; 21 other).

**RESULTS** There was extensive ATTR amyloid infiltration in the 5 atria, with loss of normal architecture, vessels remodeling, capillary disruption, and subendocardial fibrosis. Echo speckle tracking in 906 patients with ATTR-CM demonstrated increased atrial stiffness (median [25th-75th quartile] 1.83 [1.15-2.92]) that remained independently associated with prognosis after adjusting for known predictors (lnLA stiff: HR: 1.23; 95% CI: 1.03-1.49; $P = 0.029$). There was substantial impairment of the 3 phasic functional atrial components (reservoir 8.86% [5.94%-12.97%]; conduit 6.5% [4.53%-9.28%]; contraction function 4.0% [2.29%-6.56%]). Atrial contraction was absent in 22.1% of patients whose electrocardiograms showed sinus rhythm (SR) "atrial electromechanical dissociation" (AEMD). AEMD was associated with poorer prognosis compared with patients with SR and effective mechanical contraction ($P = 0.0018$). AEMD conferred a similar prognosis to patients in atrial fibrillation.

**CONCLUSIONS** The phenotype of ATTR-CM includes significant infiltration of the atrial walls, with progressive loss of atrial function and increased stiffness, which is a strong independent predictor of mortality. AEMD emerged as a distinctive phenotype identifying patients in SR with poor prognosis. (J Am Coll Cardiol Img 2022;15:17–29)


From the [a]Cardiology University Department, Heart Failure Unit, IRCCS Policlinico San Donato, San Donato Milanese, Milan, Italy; [b]Department for Biomedical Sciences for Health, University of Milano, Milan, Italy; [c]Tuscan Regional Amyloid Center, Careggi University Hospital (AOUC), Florence, Italy; [d]National Amyloidosis Centre, University College London, Royal Free Campus, London, United Kingdom; [e]Barts Heart Centre, St Bartholomew's Hospital, West Smithfield, London, United Kingdom; [f]Eastman Dental Institute, University College London, Grays Inn Road, London, United Kingdom; [g]Academic Hospital S. Orsola-Malpighi, Bologna, Italy; [h]University Cardiological Center, University of Ferrara, Italy; and the [i]Maria Cecilia Hospital, GVM Care & Research, Cotignola (RA), Italy. *Drs Bandera, Martone, Gillmore, and Fontana contributed equally to this work.

ISSN 1936-878X https://doi.org/10.1016/j.jcmg.2021.06.022

**ABBREVIATIONS AND ACRONYMS**

**ATTR-CM** = transthyretin amyloid cardiomyopathy

**EMB** = endomyocardial biopsy

**hATTR** = hereditary ATTR amyloidosis

**HF** = heart failure

**LA** = left atrium

**LAS** = left atrium strain

**LV** = left ventricle

**MAPSE** = mitral annular plane systolic excursion

**MCF** = myocardial contraction factor

**PASP** = pulmonary artery systolic pressure

**ROI** = region of interest

**TAPSE** = tricuspid annular plane systolic excursion

**wtATTR** = wild-type transthyretin

Transthyretin amyloid cardiomyopathy (ATTR-CM) is a restrictive cardiomyopathy caused by extracellular deposition of amyloid fibrils derived from plasma transthyretin. It is most commonly nonhereditary, associated with the deposition of wild-type (wt) ATTR, but there are numerous transthyretin gene variants associated with hereditary (h) ATTR forms. Advances in imaging techniques (1-4) have led to validation of nonbiopsy diagnostic criteria for ATTR-CM (4,5), underscoring a recent exponential rise in diagnosis of ATTR-CM throughout the world (6). ATTR-CM has emerged as a much underdiagnosed and under-recognized cause of heart failure (HF) (7).

Studies in patients with cardiac ATTR amyloidosis have focused predominantly on the functional and structural consequences of amyloid infiltration within the ventricles (8,9), causing biventricular wall thickening with nondilated chambers, systolic and diastolic dysfunction, and low cardiac output (10,11). By contrast, assessment of the atria has focused mainly on atrial dimensions. Left atrial (LA) dimension is generally considered to be an adequate measure of the cumulative effect of LV filling pressure over time, being a marker of severity and chronicity of diastolic dysfunction, and resulting in elevation of LA pressure.

However, measurement of LA dimension does not provide information on atrial function, which is emerging as a key component of overall cardiac performance in various cardiac disorders (12). Echo-speckle tracking now has an established role in the characterization of atrial function (13) and can assess the ability of the atria to expand during ventricular systole (reservoir function), the early-diastolic emptying (conduit function), the atrial shortening (atrial contraction), and—when associated with the estimation of LV pressures—the resistance to deformation of the LA (LA stiffness) (14). Preliminary findings in cardiac amyloidosis have demonstrated impaired atrial systolic contraction (15) but also loss of reservoir function, resulting in an atrium that acts merely as a conduit throughout the cardiac cycle (16,17). To date, only small retrospective speckle-tracking studies have been conducted in ATTR amyloidosis, and along with little in the way of histological evaluation of the atrial wall, the significance of atrial infiltration, remodeling, and dysfunction in the pathophysiology of cardiac ATTR amyloidosis is not clear.

The aims of the current study were to characterize the spectrum of changes in LA structure in postmortem specimens of patients with ATTR-CM, the functional consequences of amyloid deposition on LA stiffness, and mechanics in a large cohort of patients with cardiac ATTR amyloidosis, using echocardiographic speckle tracking, and to assess the association between atrial functional parameters and clinical outcomes.

## METHODS

**PATIENT POPULATION.** Patients referred to the National Amyloidosis Centre (NAC), Royal Free Hospital, London, United Kingdom, between 2000 and 2019, in whom ATTR-CM was confirmed on the basis of validated diagnostic criteria (5) were invited to participate in a prospective registry with protocolized clinical follow-up program comprising systematic evaluation of cardiac parameters and survival. Clinical, biochemical, and imaging data were retrospectively analyzed for this study. Briefly, the diagnosis of ATTR-CM was established on the basis of the following criteria: presence of symptoms of HF, together with an echocardiogram consistent with amyloidosis and either: 1) direct endomyocardial biopsy (EMB) proof of ATTR amyloid; 2) presence of ATTR amyloid in an extracardiac biopsy along with cardiac uptake on 99mTechnetium labeled 3,3-diphosphono-1,2-propanodicarboxylic acid (99mTc-DPD) scintigraphy; or 3) Perugini grade 2 or 3 cardiac uptake on 99mTc-DPD scintigraphy in the absence of a monoclonal immunoglobulin disorder (5). The transthyretin (TTR) gene was sequenced in all participants. Patients who had received disease-modifying therapy, including liver transplantation for hATTR amyloidosis, or a TTR-lowering therapy (within the context of a clinical trial) were excluded from the study.

The atria from 5 explanted hearts of patients with ATTR-CM (3 with wtATTR-CM and 2 with hATTR-CM) were sampled. Patients were managed in accordance

The authors attest they are in compliance with human studies committees and animal welfare regulations of the authors' institutions and Food and Drug Administration guidelines, including patient consent where appropriate. For more information, visit the Author Center.

Manuscript received November 30, 2020; revised manuscript received May 20, 2021, accepted June 1, 2021.

**TABLE 1 Clinical Characteristics in the 3 Subgroups: SR With LAMC, SR Without LAMC, and Non-SR**

| | SR With LAMC (n = 439 [48.5%]) | SR Without LAMC (n = 125 [13.8%]) | Non-SR (n = 342 [37.7%]) | *P* Value |
|---|---|---|---|---|
| Age, y | 74 ± 8.5 | 75.3 ± 8.2 | 76.9 ± 6.8 | <0.001[a] |
| Male | 353 (80.4) | 104 (83.2) | 315 (92.2) | <0.001 |
| BSA, kg/m$^2$ | 1.86 ± 0.19 | 1.86 ± 0.19 | 1.90 ± 0.17 | 0.007[a] |
| Race | | | | <0.001 |
| Black | 128 (29.1)[a] | 41 (32.8)[b] | 67 (19.7) | |
| White | 283 (64.5)[a] | 76 (60.8)[b] | 265 (77.5) | |
| Other | 19 (4.4)[a] | 5 (4.0)[b] | 2 (0.5) | |
| Missing | 9 (2.0) | 3 (2.4) | 8 (2.3) | |
| Genotype | | | | <0.001 |
| Wildtype | 236 (53.7)[a] | 61 (48.8)[b] | 254 (74.3) | |
| T60A | 59 (13.4)[a] | 13 (10.4) | 21 (6.1) | |
| V122I | 129 (29.4)[a] | 48 (38.4)[b] | 64 (18.7) | |
| Other variants | 15 (3.5) | 3 (2.4) | 3 (0.9) | |
| NYHA functional class | | | | 0.005 |
| 1 | 51 (11.6)a | 7 (5.6) | 17 (5.0) | |
| 2 | 313 (71.3) | 92 (73.6) | 241 (70.5) | |
| 3 | 74 (16.9) | 25 (20.0) | 80 (23.4) | |
| 4 | 1 (0.2) | 1 (0.8) | 4 (1.2) | |
| Biomarker stage | | | | <0.001 |
| Grade 1 | 259 (59.0)[a,c] | 54 (43.9) | 113 (32.8) | |
| Grade 2 | 124 (28.2)[a] | 40 (32.5) | 164 (47.7) | |
| Grade 3 | 51 (11.6)[a,c] | 29 (23.6) | 64 (18.6) | |
| Missing data | 5 (1.2) | 0 (0.0) | 3 (0.9) | |
| Heart rate, beats/min | 70 ± 12 | 75 ± 15 | 75 ± 15 | <0.001[a,c] |
| Systolic blood pressure, mmHg | 127 ± 19 | 125 ± 18 | 121 ± 17 | <0.001[a] |
| Diastolic blood pressure, mmHg | 74 ± 10 | 74 ± 11 | 74 ± 11 | 0.911 |
| NT-proBNP, ng/L | 2,064 (1,108-3,755) | 3,696 (1,937-6,484) | 3,856 (2,287-6,614) | <0.001[a,c] |
| Troponin, ng/mL | 53 (35-81) | 71 (48-104) | 64 (42-95) | <0.001[a,b,c] |
| GFR, mL/min per 1.73 m$^2$ | 63 (50-79) | 56 (44-67) | 56 (46-70) | <0.001[a,c] |
| 6MWT, meters | 348 ± 138 | 310 ± 140 | 309 ± 136 | 0.010[a,c] |
| 6MWT, % of predicted | 77 ± 27 | 71 ± 27 | 66 ± 26 | 0.009[a] |
| Antiplatelet treatment | 83 (19) | 19 (15) | 24 (7) | <0.001[a,b] |
| Anticoagulants | 114 (26) | 34 (27) | 196 (57) | <0.001[a,b] |
| Warfarin | 65 (15) | 16 (13) | 137 (40) | <0.001[a,b] |
| DOAC | 49 ± 11 | 18 (14) | 59 (17) | 0.225 |
| ACEIs | 154 (44) | 49 (46) | 143 (42) | 0.911 |
| ARBs | 63 (18) | 18 (17) | 52 (17) | 0.877 |
| β-blockers | 167 (48) | 52 (49) | 179 (58) | 0.040[a] |
| MRA | 82 (24) | 24 (22) | 93 (30) | 0.124 |
| Loop diuretics | 226 (65) | 79 (74) | 253 (81) | <0.001[a] |
| Thiazide diuretics | 15 (4) | 8 (7) | 22 (7) | 0.245 |

Values are mean ± SD, n (%), or median (25th-75th percentiles). The *P* values refer to comparison above the 3 subgroups. The *P* values for pairwise comparison. [a]$P < 0.05$ for SR with LAMC vs non-SR. [b]$P < 0.05$ for SR without LAMC vs non-SR. [c]$P < 0.05$ for SR with LAMC vs SR without LAMC.

ACEI = angiotensin-converting enzyme inhibitor; ARB = angiotensin receptor blocker; BSA = body surface area; DOAC = direct oral anticoagulants; GFR = glomerular filtration rate; LAMC = left atrial mechanical contraction; MRA = mineralcorticoid receptor antagonist; NT-proBNP = N-terminal pro-hormone brain natriuretic peptide; NYHA = New York Heart Association; 6MWT 6-minute walk test; SR = sinus rhythm.

with the Declaration of Helsinki and provided written informed consent (ref: 06/Q0501/42 and 79/2014/U/Sper, Royal Free Ethics Committee, London, United Kingdom, and AOU of Bologna, Italy).

**HISTOLOGIC ANALYSIS.** The atria samples were fixed in neutral buffered formalin and processed into a paraffin blocks (FFPE) for routine histology, Congo red staining and immunohistochemistry (IHC); IHC was performed using commercially available monospecific antibodies against human serum AA, kappa, lambda, and prealbumin (transthyretin) (Agilent Technologies), and NKx2.5. Staining was performed on a manual platform, with ImmPRESS detection kits (Vector Laboratories) and a metal enhanced DAB substrate kit for visualizing the immune compound. Ready-to-use antibodies against vWF, CD31, CD45,

**TABLE 2 Echocardiographic Findings in the 3 Subgroups: SR With LAMC, SR Without LAMC, and Non-SR**

| | SR With LAMC (n = 439 [48.5%]) | SR Without LAMC (n = 125 [13.8%]) | Non-SR (n = 342 [37.7%]) | *P* Value |
|---|---|---|---|---|
| IVSD (mm) | 16.7 ± 2.4 | 16.8 ± 2.2 | 16.9 ± 2.3 | 0.262 |
| PWTD (mm) | 16.4 ± 2.4 | 16.6 ± 2.2 | 16.3 ± 2.5 | 0.226 |
| LVM (g) | 307.0 ± 79.8 | 297.0 ± 79.1 | 318.2 ± 74.2 | <0.001[a,b] |
| RWT | 0.76 ± 0.17 | 0.79 ± 0.15 | 0.76 ± 0.17 | 0.016[c] |
| LVEDD (mm) | 43.4 ± 5.8 | 41.7 ± 5.5 | 44.0 ± 5.8 | <0.001[b,c] |
| LVEDD indexed (mm/m$^2$) | 23.4 ± 3.1 | 22.5 ± 2.9 | 23.1 ± 2.9 | 0.006[c] |
| MWT (mm) | 16.2 ± 2.3 | 16.7 ± 2.1 | 16.6 ± 2.3 | 0.242 |
| LVEDV (mL) | 77.0 ± 25.9 | 69.3 ± 22.2 | 77.7 ± 26.3 | 0.008[b,c] |
| LVEDV indexed (mL/m$^2$) | 41.3 ± 12.7 | 37.4 ± 10.6 | 40.6 ± 12.7 | 0.017[c] |
| LVESV (mL) | 38.5 ± 17.7 | 38.6 ± 17.2 | 42.8 ± 18.5 | <0.001[a] |
| LVESV indexed (mL/m$^2$) | 20.6 ± 8.9 | 20.8 ± 8.4 | 22.4 ± 9.4 | 0.013[a] |
| SV (mL) | 38.6 ± 13.7 | 30.7 ± 11.0 | 34.9 ± 13.4 | <0.001[a,b,c] |
| SV indexed (mL/m$^2$) | 20.8 ± 6.8 | 16.6 ± 5.6 | 18.2 ± 6.6 | <0.001[a,c] |
| LVEF (%) | 50.6 ± 10.4 | 45.0 ± 10.8 | 45.5 ± 11.1 | <0.001[a,c] |
| E (cm/s) | 83.8 ± 20.7 | 86.8 ± 19.4 | 84.8 ± 18.7 | 0.188 |
| DTE (ms) | 187.2 ± 55.7 | 163.6 ± 57.3 | 177.7 ± 52.4 | <0.001[a,c] |
| E/A | 2.11 ± 1.6 | - | - | - |
| Mean e' (cm/s) | 5.1 ± 1.5 | 5.3 ± 1.7 | 5.9 ± 1.7 | <0.001[a,b] |
| E/e' | 17.4 ± 6.0 | 17.8 ± 6.1 | 15.6 ± 6.0 | <0.001[b] |
| RA area (cm$^2$) | 22.0 ± 5.7 | 24.2 ± 5.8 | 27.1 ± 6.6 | <0.001[a,b,c] |
| RA area indexed (cm$^2$/m$^2$) | 12.0 ± 3.0 | 13.1 ± 2.9 | 14.2 ± 3.4 | <0.001[a,b,c] |
| MAPSE (mm) | 9.0 ± 6.7 | 7.6 ± 2.6 | 7.6 ± 2.5 | <0.001[a,c] |
| TAPSE (mm) | 16.7 ± 4.5 | 13.6 ± 4.4 | 12.8 ± 3.7 | <0.001[a,c] |
| PASP (mm Hg) | 42.7 ± 12.3 | 45.2 ± 9.4 | 43.3 ± 9.6 | 0.056 |
| TAPSE/PASP (mm/mm Hg) | 0.43 ± 0.22 | 0.30 ± 0.12 | 0.31 ± 0.14 | <0.001[a,c] |
| Tricuspid S' (cm/s) | 11.3 ± 3.1 | 9.0 ± 2.6 | 9.1 ± 2.5 | <0.001[a,c] |
| MCF (%) | 15.9 ± 5.9 | 13.9 ± 5.0 | 14.3 ± 5.2 | <0.001[a,c] |
| LVLS (%) | -12.0 ± 3.7 | -9.4 ± 3.5 | -10.1 ± 3.3 | <0.001[a,c] |
| SABr | 5.35 ± 6.63 | 4.78 ± 6.53 | 5.20 ± 7.16 | 0.611 |
| RALS | 1.70 ± 1.15 | 1.96 ± 1.61 | 1.82 ± 1.30 | 0.310 |
| Significant MR | 118 (26.9) | 43 (34.4) | 133 (38.9) | 0.002[a] |
| Significant TR | 107 (24.4) | 52 (41.6) | 128 (37.2) | <0.001[a,c] |
| LA diameter (mm) | 43.7 ± 5.5 | 44.2 ± 6.0 | 46.6 ± 5.4 | <0.001[a,b] |
| LA area (cm$^2$) | 25.2 ± 4.9 | 26.0 ± 5.2 | 28.1 ± 5.9 | <0.001[a,b] |
| LA area indexed (cm$^2$/m$^2$) | 13.7 ± 2.8 | 14.0 ± 2.7 | 14.8 ± 3.0 | <0.001[a] |
| LAS reservoir (%) | 11.2 (8.1-15.3) | 7.3 (5.2-10.9) | 6.9 (4.7-9.6) | <0.001[a,c] |
| LAS conduit (%) | 6.5 (4.5-9.3) | - | - | |
| LAS contraction (%) | 4.1 (2.3-6.6) | - | - | |
| LA stiffness (1/%) | 1.47 (0.98-2.39) | 2.30 (1.40-3.54) | 2.16 (1.38-3.54) | <0.001[a,c] |
| ln LA stiffness | 0.38 (0.02-0.87) | 0.83 (0.34-1.26) | 0.77 (0.32-1.26) | <0.001[a,c] |

Values are as mean ± SD, n (%), or median (25th-75th percentiles). The *P* values refer to comparison above the 3 subgroups. The *P* values for pairwise comparison. [a]$P < 0.05$ for SR with LAMC vs non-SR. [b]$P < 0.05$ for SR without LAMC vs non-SR. [c]$P < 0.05$ for SR with LAMC vs SR without LAMC.

DTE = E deceleration time; IVSD = diastolic interventricular septum; LA = left atrium; LAS = peak left atrium strain; LS = longitudinal strain; LVEDD = left ventricle end-diastolic diameter; LVEDV = left-ventricle end diastolic volume; LVEF = left-ventricle ejection fraction; LVESV = left-ventricle end systolic volume; LVM = left ventricle mass; MAPSE = mitral annular plane systolic excursion; MCF = myocardial contraction fraction; MR = mitral regurgitation; MWT = maximal wall thickness; PASP = pulmonary artery systolic pressure; PWTD = diastolic posterior wall thickness; RA = right atrium; RALS = relative apical longitudinal strain; RWT = relative wall thickness; SABr = systolic apex to base ratio; SR = sinus rhythm; SV = stroke volume; TAPSE = tricuspid annular plane systolic excursion; TR = tricuspid regurgitation.

and CD68 (Leica Microsystems) were carried out using a BOND Max immunostainer (Leica Biosystems) and DAB refine kit. Amyloid was laser captured for proteomic analysis to confirm IHC staining. Proteomic analysis was processed on the Thermo Scientific Q-Exactive Plus Orbitrap (ThermoFisher). Data were analyzed using Mascot software and the SWISS-PROT human database. All IHC slides and proteomic analysis were interpreted blind to any clinical details by 2 independent reporters; IHC results were compared with data obtained from proteomic analysis: in particular, with respect to positive identification of the amyloid fibril protein.

**ECHOCARDIOGRAPHY.** All echocardiograms were reviewed by experienced operators and analyzed according to guidelines, as previously reported (10). For the purpose of our analysis, we considered valvular regurgitation to be clinically significant if at least mild to moderate or greater.

**LEFT ATRIAL ASSESSMENT.** Left atrial dimensions were reported as parasternal long-axis diameter, absolute, and body surface area (BSA)-indexed, 4-chamber area. LA speckle tracking analysis was performed using EchoPAC software Version 203 (GE Healthcare), according to the current consensus document (18). Briefly, nonforeshortened 2-dimensional apical 4-chamber view was used to define a 3-mm thickened wall region of interest (ROI) along the LA. The LA contour was extrapolated excluding pulmonary veins and LA appendage. Quality control check was performed to reject cases with significant (greater than one-third of LA contour) drop out of atrial wall. Zero-baseline was defined as ventricular end-diastole, using the R-R cycle for analysis. LA myocardial deformation was assessed as global longitudinal strain obtained with the endocardial curve of the ROI. Reservoir, contraction, and conduit phase were studied respectively as LA strain (LAS) reservoir = peak value at the onset of LV filling, LAS contraction = peak value at the onset of atrial contraction (for subjects on sinus rhythm), and LAS conduit = difference between LAS reservoir and LAS contraction (for subjects on sinus rhythm). LA stiffness was calculated as the ratio between E/e' and LAS reservoir, in which e' is the mean value between lateral and septal e' (14).

**STATISTICAL ANALYSIS.** All mortality data were obtained via the UK Office of National Statistics. The mortality endpoint was defined as time to death from baseline for all deceased patients and time to Censor date—April 24, 2019—from baseline among the remainder. Baseline was the time of diagnosis. The 3 genotypic subgroups of interest were wtATTR-CM, V122I-associated hereditary ATTR-CM (V122I-hATTR-CM), and T60A-associated hereditary ATTR-CM (T60A-hATTR-CM).

As a number of the numeric variables had skewed distributions, a Kruskal-Wallis test was used to

**FIGURE 1 Histologic Findings in Postmortem Atria**

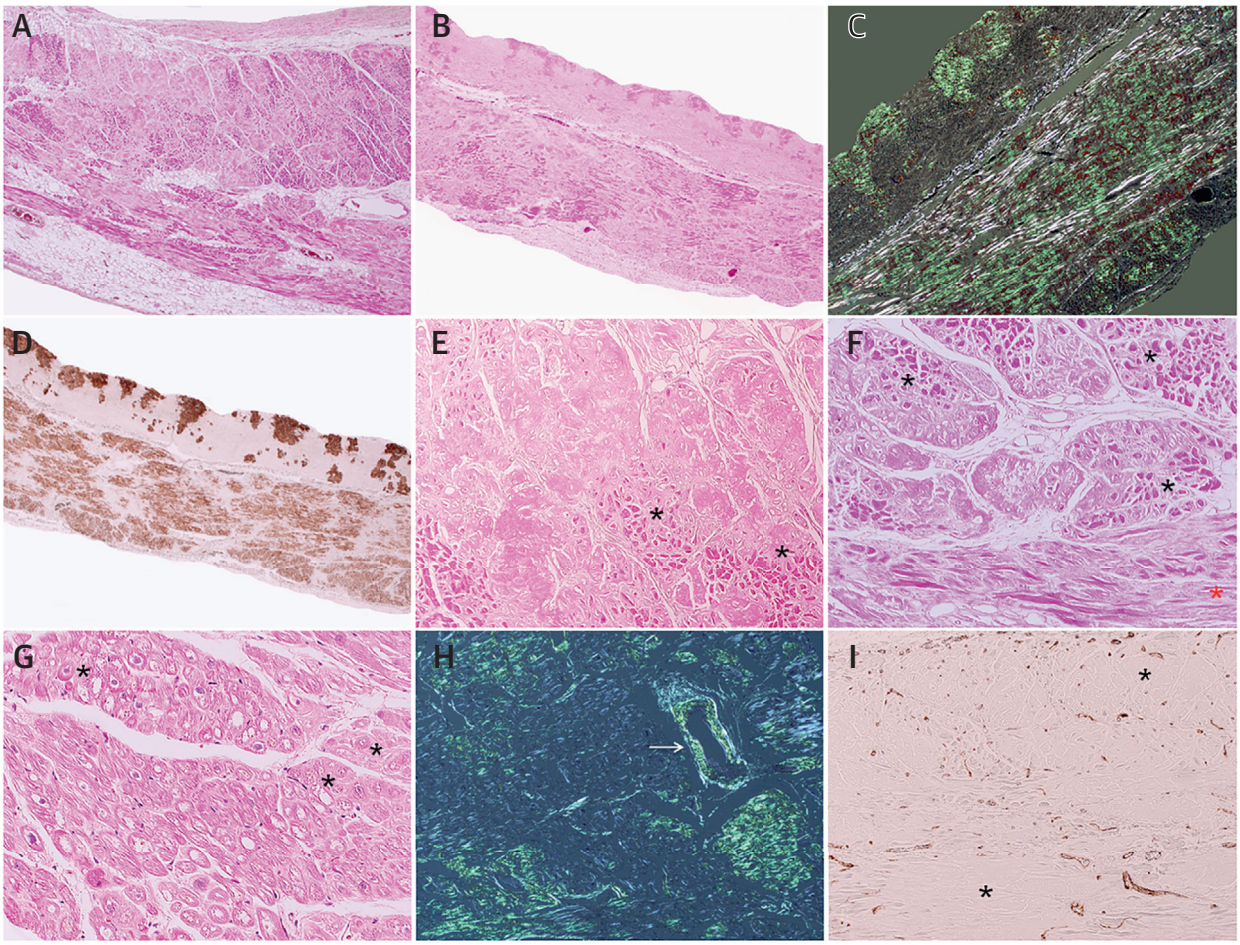


Atrial sample histology from native hearts of a 71-year-old man with V122I-associated hATTR-CM **(A,E,F)**, of a 85-year-old-man with wtATTR-CM **(B,C,D,H)**, of a 51-year-old man transplanted for wtATTR-CM **(G)**, and of a 54-year-old man with E89Q-associated hATTR-CM **(I)**. **(A-D)** Scanner magnification shows the extensive eosinophilic amyloid deposits distributed throughout subendocardium and myocardial interstitium in the form of both streaks along myocytes and large accumulations **(A)** H&E 25x; **(B)** H&E 25x; **(C)** Congo red green birefringence 25x; **(D)** TTR immunohistochemistry, 25x. **(E,F)** H&E, 100x highlight nodular amyloid deposits responsible for attenuation and atrophy **(black asterisks)** or thinning out **(red asterisks)** of myocytes. **(G)** At high power (H&E, 200x), cytoplasmic vacuolization of myocytes are evident. (H) Congo red, 100x: green amyloid deposits are present within the wall of a small intramural artery **(white arrow)**. **(I)** CD31 immunostaining shows decreased or absent capillary network within nodular amyloid aggregates **(asterisks)** (100x). hATTR-CM = hereditary transthyretin amyloid cardiomyopathy; H&E = hematoxylin and eosin; wtATTR-CM = wild-type transthyretin amyloid cardiomyopathy.

compare the distributions of each of the numeric variables at baseline in the subgroups. A significant result was followed by Bonferroni-corrected Mann-Whitney pairwise comparisons to establish where the differences lay. For categorical variables, chi-square test was used followed by z-test with Bonferroni correction for pairwise comparison because of the large sample size. Correlation among nonparametric variables was explored using Spearman test.

Survival was evaluated with Cox proportional hazards regression analysis, providing estimated HRs with 95% CIs and Kaplan-Meier curves. Twenty echocardiographic variables were selected based upon clinical relevance and previous report (10): interventricular septum in diastole (IVSd), relative wall thickness (RWT), stroke volume indexed, LV ejection fraction (EF), LV longitudinal strain (LS), E/e', myocardial contraction factor (MCF), mitral annular plane systolic excursion (MAPSE), significant mitral regurgitation (MR), significant tricuspid regurgitation (TR), right-atrium area (RAA) index, tricuspid annular plane systolic excursion (TAPSE),

**TABLE 3 LA Mechanics and Stiffness in ATTR-CM Genotypes**

| | wtATTR-CM (n = 554 [62%]) | T60A-ATTR-CM (n = 97 [11%]) | V122A-ATTR-CM (n = 242 [27%]) | *P* Value |
|---|---|---|---|---|
| LAS reservoir (%) | 9.0 (6.0-13.0) | 11.4 (7.0-15.7) | 8.0 (5.3-10.9) | 0.001[a,b,c] |
| LAS conduit (%) | 6.6 (4.5-9.3) | 7.0 (4.7-10.0) | 6.1 (4.2-8.2) | 0.078 |
| LAS contraction (%) | 4.1 (2.3-7.0) | 5.0 (2.8-8.4) | 3.1 (1.6-5.0) | 0.001[b,c] |
| LA stiffness (1/%) | 1.72 (1.10-2.83) | 1.67 (0.87-2.70) | 2.12 (1.34-3.29) | <0.001[b,c] |

Values are median (25th-75th percentiles). The *P* values refer to comparison above the 3 subgroups. The *P* values for pairwise comparison. [a]$P < 0.05$ for wtATTR-CM vs T60A-ATTR-CM. [b]$P < 0.05$ for T60A-ATTR-CM vs V122A-ATTR-CM. [c]$P < 0.05$ for wtATTR-CM vs V122A-ATTR-CM.

Abbreviations as in Tables 1 and 2.

TAPSE/pulmonary artery system pressure (PASP), LA diameter, LA area, LA area indexed, LAS reservoir, LAS conduit, LAS contraction, and ln LA stiffness. The proportional hazards assumption was checked and confirmed. The echocardiographic variables were first explored with univariate Cox regression analysis. The variables that were statistically significant predictors of outcome on simple Cox regression analysis were entered into a multivariable Cox proportional hazards analysis to determine which covariates were independent predictors of mortality. Because LA stiffness was introduced in the model, LAS reservoir and E/e' were not included for the collinearity among variables. The model was also adjusted for heart rate, cardiac rhythms, genotypes, and time of diagnosis (the variable was categorized as before or after February 15, 2015, which was the median date of diagnosis). Possible collinearity among candidate predictors was assessed using variance-inflation factors with threshold equal to 5.

After verifying the required statistical assumptions, a linear regression for LA reservoir function was assessed with diastolic variables to understand the interplay between LA mechanics and LV diastolic function.

All data were analyzed using Stata software (StataCorp LLC). A significance level of 0.05 was used for all hypothesis tests unless otherwise stated.

## RESULTS

**CHARACTERISTICS OF THE OVERALL COHORT.** The echocardiograms of 1,240 patients with ATTR-CM were retrospectively analyzed by speckle-tracking analysis of LA strain. A total of 906 patients had LA strain analysis in line with current consensus guidelines (18). In 334 (26.9%) patients, LA strain analysis was not feasible because of inadequate acoustic windows, excessive breathing-related cardiac motion, LA foreshortening, or significant atrial wall dropout. The final cohort (Tables 1 and 2) comprised 906 patients, 551 (62.3%) with wtATTR-CM (age 77 ± 7 years, male 95.3%), 241 (26.6%) with V122I-associated hATTR-CM (age 76 ± 7 years, male 70.1%), 93 (10.3%) with T60A-associated hATTR-CM (age 66 ± 7 years, male 65.5%), 21 (2.3%) with non-V122I, non-T60A-associated hATTR-CM (age 62 ± 12 years, male 81%). The patients with non-V122I, non-T60A-associated hATTR-CM had the following TTR variants: G47V, V30M, S77Y, I73V, A120S, D39V, E89K, H90D, I107V, F33I, V20I.

**HISTOLOGIC FINDINGS.** The 5 patients with ATTR-CM whose explanted hearts underwent histological study were men, average age 61 (range 51 to 88) years; 3 had wtATTR, 2 hATTR (V122I, E89Q). Figure 1 summarizes the major histological findings. There was extensive ATTR amyloid deposition within the myocardial interstitium and subendocardium in all samples. Proteomic analysis confirmed the amyloid deposits to be ATTR type and also identified atrial natriuretic peptide in 3 of 5 patients although with low Mascot score. Amyloid deposits were severe and diffusely distributed in 3 cases and moderate and scattered in multifocal areas in 2 cases. In all specimens, the myocardial interstitial deposits were perimyocite and, for the most part, aggregated in nodules replacing normal tissue; in the subendocardium, there were nodular deposits within fibrous tissue. Amyloid vascular deposits were also seen in all samples, both in small intramural vessels and in subepicardial arteries and veins, with a focal distribution in 4 cases and multifocal in 1. In addition, phenotypic modulation and vascular remodeling in arteries of all samples were found as confirmed by high level of NKX2-5 expression in intimal and medial layers. NKX2-5 expression is not present in healthy adult vessels, as expression of NKX2-5 is associated with phenotypic modulation of vascular smooth-muscle cells and endothelial cells of vessels undergoing vascular remodeling in pathology. Mild-to- moderate subendocardial fibrosis was present in all samples; myocardial interstitial fibrosis was absent.

Widespread ATTR amyloid deposition was associated with histological myocardial remodeling in all samples, including myocyte morphological changes such as attenuation and atrophy and thinning, which was distributed diffusely in 3 specimens and was multifocal in 2. Focal and multifocal areas with reactive hypertrophied or vacuolated myocytes were also noted. Acute myocyte injury was absent in all samples.

CD31 and von Willebrand factor VIII immunostaining revealed decreased capillary network in all samples, with diffuse distribution in 3 specimens,

**FIGURE 2** **Left Atrial Reservoir, Conduit, and Contraction Function in Patients With ATTR-CM According to Increasing Left Atrial Stiffness**

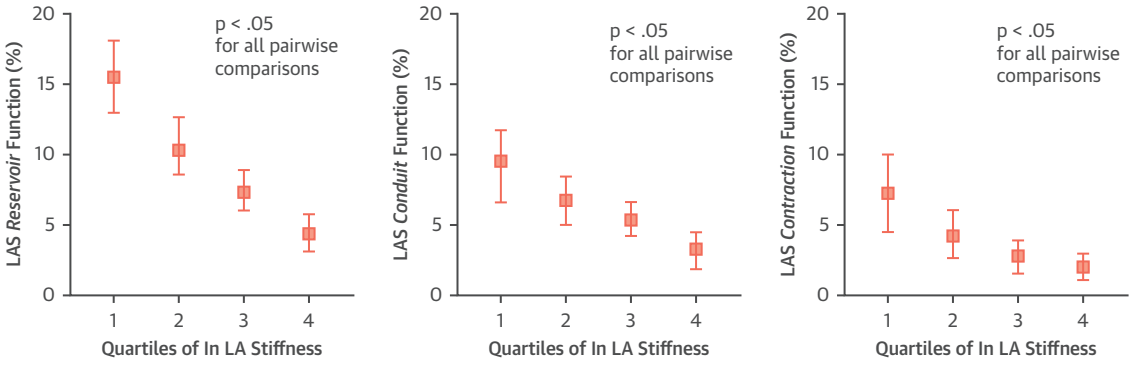


Median with IQR is represented. The *P* value refers to adjusted pairwise comparisons. ATTR-CM = transthyretin amyloid cardiomyopathy; LA = left atrium; LAS = LA strain.

multifocal in 1, and focal in 1. There were no significant inflammatory infiltrates, with only 2 samples showing mild inflammation comprising interstitial macrophages and few lymphocytes.

**STRAIN-DERIVED LA STRUCTURE AND FUNCTION.** LA stiffness was significantly increased in patients with cardiac amyloidosis (LA stiffness (median [25th to 75th quartile], 1.83 [1.15-2.92]) compared with normal reference range (mean ± SD, 0.21 ± 0.1) (19), and this was confirmed across the 3 predominant genotypes (wtATTR-CM [median, 25th to 75th quartile, 1.72 [1.10-2.83], T60A-ATTR-CM 1.67 [0.87-2.70] and V122I-ATTR-CM 2.12 [1.34-3.29] Kruskal-Wallis; $P = 0.001$, wtATTR-CM vs V122I-ATTR-CM; $P = 0.003$, T60A-ATTR-CM vs V122I-ATTR-CM; $P = 0.024$, other comparison not significant). The amyloidosis phenotype was also characterized by significant reduction of the 3 atrial functional components (LAS reservoir [median, 25th to 75th quartile] 8.86 [5.94-12.97], LAS conduit 6.5 [4.53-9.28], and LAS contraction 4.0 [2.29-6.56]), with significant differences across the 3 main genotypes. The most impaired overall functional pattern was present in patients with V122I genotype (**Table 3**). There was a weak correlation between the lnLA stiffness and atrial dilatation (LA indexed area) (Spearman $r^2 = 0.036$; $P < 0.001$). Increased LA stiffness was associated with a progressive reduction in the reservoir, conduit and contraction function (**Figure 2**). Linear regression for LAS reservoir showed very low $r$ for all LV diastolic variables (Supplemental Table 2).

Among the 906 patients, 564 (62.2%) patients were in sinus rhythm (SR group), and 342 patients (37.8%) were not (non-SR group), comprising 313 (91.5%) in AF and 29 (8.5%) in atrial flutter or tachycardia.

Of the patients in SR, 439 (77.8%) patients had evidence of atrial contraction on LA strain analysis (SR with LA mechanical contraction [LAMC] group) and 125 (22.2%) patients did not show evidence of atrial contraction (SR without LAMC group) (**Figure 3**). These groups were defined based only on the presence or absence of atrial contraction on LA strain analysis. Patients in the SR without LAMC group did not show evidence of A wave or the A wave was very low (<20 cm/s) on transmitral Doppler analysis. The clinical phenotypes (as identified by the UK National Amyloidosis Centre [NAC] staging system, N-terminal pro B-type Natriuretic Peptide [NT-proBNP], troponin, estimated glomerular filtration rate [eGFR], and 6-minute walk test [6MWT]) of SR without LAMC and non-SR patients were similar and significantly worse than patients in SR with LAMC (**Table 1**). Patients with SR without LAMC had more severe systolic dysfunction compared with patients in SR with LAMC. LA-indexed area of SR with LAMC patients was significantly reduced only when compared with the non-SR group (**Table 2**). By contrast, LAS reservoir and LA stiffness were significantly and similarly impaired in SR without LAMC and non-SR patients. Fifty-seven percent of non-SR patients were on anticoagulants, whereas both SR subgroups showed similar prevalence of approximately 26% to 27%.

**STRAIN DERIVED LA STRUCTURE, FUNCTION, AND PROGNOSIS.** At follow-up (mean 35 ± 22 months), 370 (40.8%) of 906 patients had died. Median patient survival from diagnosis by Kaplan-Meier analysis was 55 months in the overall group of SR patients, 58 and 44 in SR with LAMC and SR without LAMC, respectively, and 51 months in non-SR patients (**Figure 4**).

**FIGURE 3 Left Atrial Mechanics in Patients With SR With LAMC, SR Without LAMC, (SR Without LAMC), and Non-SR**

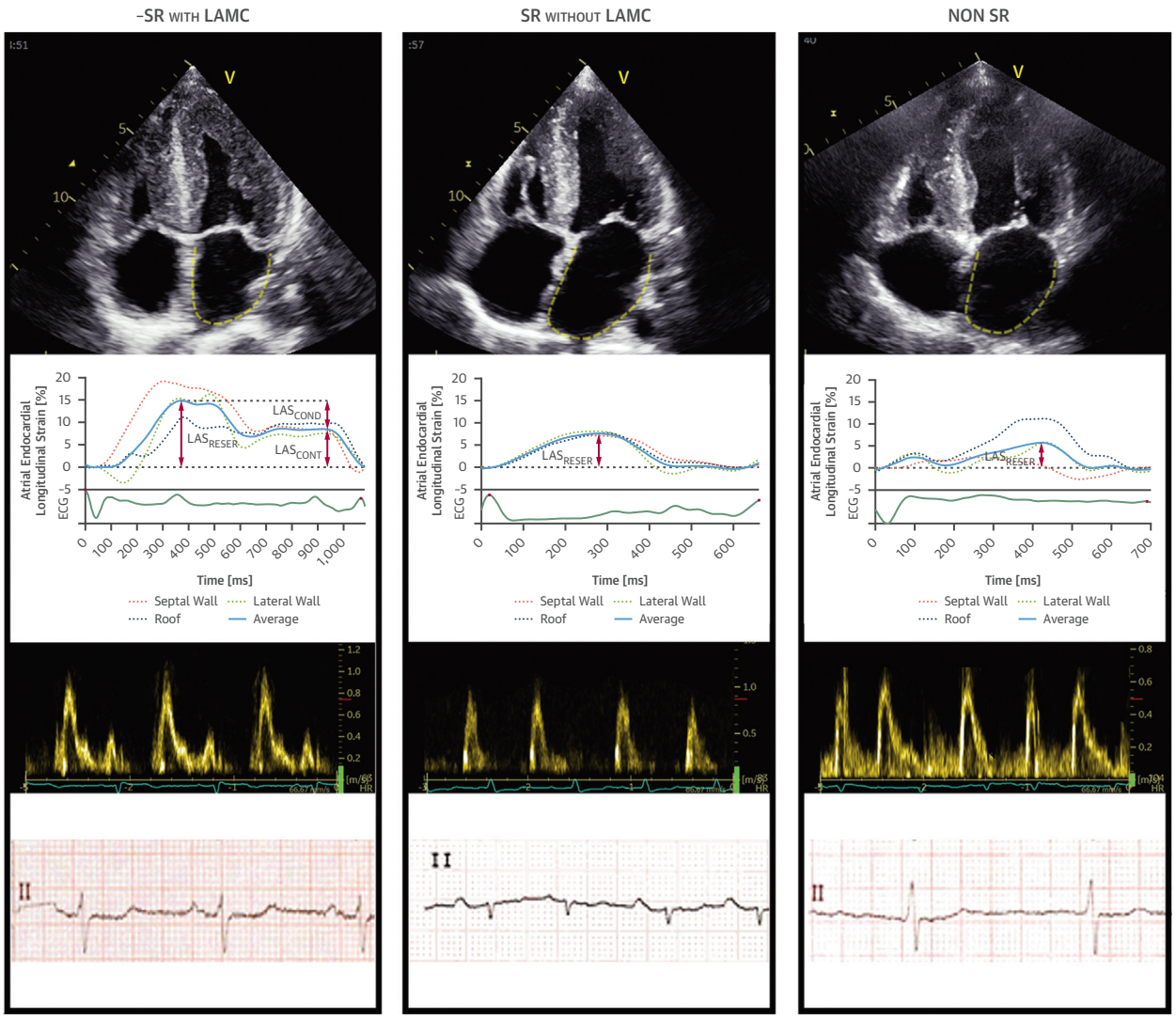


**(From top to bottom)** apical 4 chamber view showing strain endocardial trace; endocardial longitudinal strain curves with measurements of LA functional components; transmitral pulsed-wave Doppler; electrocardiographic trace. LA = left atrium; LAMC = left atrial mechanical contraction; SR = sinus rhythm.

Twenty-one echocardiographic variables, heart rate, rhythm, genotype, and the time of diagnosis were explored in the univariate Cox regression analysis (Supplemental Table 1). Ten echocardiographic variables and heart rate, cardiac rhythm, genotype, and the time of diagnosis were entered into a multivariable Cox proportional hazard analysis (**Table 4**). To avoid collinearity, and in light of a nonsignificant role in previous multivariate models (10), E/e' was not entered into the multivariate model. For all variables, the variance inflation factor was <2. The final model, combining IVSd, RWT, SVindex, LVLS, RAA index, significant MR, significant TR, TAPSE/PASP, LAA index, ln LA stiffness, heart rate, SR vs non-SR, and the time of diagnosis revealed that ln LA stiffness (HR: 1.23; 95% CI: 1.03-1.49; $P = 0.029$) remained independently associated with patient survival, together with RAA index (HR: 1.05; 95% CI: 1.01-1.10; $P = 0.033$), LVLS (HR: 1.07; 95% CI: 1.03-1.12; $P = 0.002$), significant MR (HR: 1.35; 95% CI: 1.03-1.77; $P = 0.032$), genotypes (V122I-ATTR-CM vs wtATTR-CM; HR: 1.49; 95% CI: 1.12-1.97; $P = 0.006$) and the

**FIGURE 4** **Kaplan-Meier Curves Displaying the Prognostic Impact of Left Atrial Stiffness in Patients With ATTR-CM**

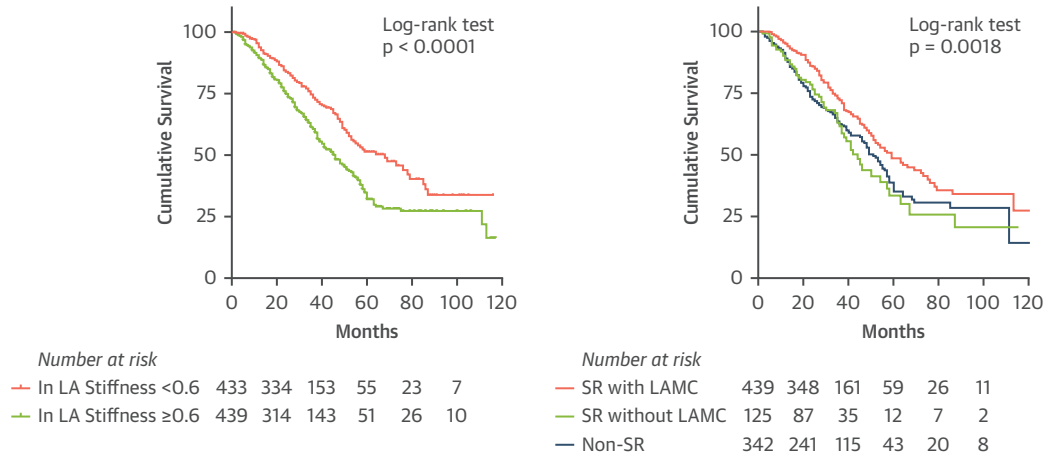


**(Left panel)** Kaplan-Meier curves displaying the differences in prognosis according with median value of In LA Stiffness. **(Right panel)** Kaplan-Meier curves displaying the differences in prognosis in patients with sinus rhythm with left atrial mechanical contraction (SR with LAMC), sinus rhythm without left atrial mechanical contraction (SR without LAMC), and non-sinus rhythm (Non-SR). LA = left atrium; LAMC = left atrial mechanical contraction; SR = sinus rhythm.

period of diagnosis (before vs after February 9, 2015; HR: 1.52; 95% CI: 1.13-2.06; $P = 0.006$).

## DISCUSSION

This is the first study to provide a systematic assessment of LA function and structure in patients with cardiac ATTR amyloidosis. The disease is characterized on histology by extensive amyloid infiltration in the atria, causing loss of normal architecture, remodeling of the vessels, capillary disruption, and upregulation of the collagen at the level of the subendocardium. Atrial infiltration by ATTR amyloid translates in significantly increased atrial stiffness, which is independently associated with reduced outcome after adjusting for all known prognostic variables (**Central Illustration**).

Abnormal stiffness of the LA myocardium is associated with reduction in the reservoir and contractile function of the atrium, with a remarkable one-fifth of patients showing an absence of contraction while remaining in SR on the electrocardiogram: ie, "atrial electromechanical dissociation" (AEMD). The prognosis of patients with AEMD was significantly poorer than for patients in SR who maintained effective mechanical contraction and was similar to those with AF.

Cardiac amyloidosis is considered an exemplar of restrictive cardiomyopathy, with ventricular diastolic dysfunction having the central role in disease pathophysiology and evolution. It has been thought that increasing LV infiltration by amyloid underlies progressive worsening of diastolic function, predominantly causing abnormal relaxation in the early stage leading to a shift of diastolic filling during late diastole (20). As amyloid accumulates, LA pressure increases producing a pseudonormal pattern on the Doppler tracing. In more advanced disease, the increase in LV myocardial stiffness causes restriction to filling with a greater rise of ventricular pressure for a small change in volume, reflected in a characteristic elevation of the E/A ratio >2. This pattern has been traditionally thought to reflect the restrictive ventricular physiology: ie, rapid filling of a very stiff LV. However, an elevated E/A ratio could also reflect a decrease of atrial contractile properties (21), resulting from a primary LA systolic failure caused by the increased stiffness produced directly by atrial amyloid infiltration. Although it may be difficult to determine whether a diminutive transmitral A wave is a function of the true atrial dysfunction or of restrictive LV pathophysiology, it is likely that there is at least a component of primary atrial dysfunction. This hypothesis is supported by the results from our study, in which we report extensive amyloid infiltration of TTR type in the atrial walls of 5 explanted hearts obtained from patients with ATTR-CM. In the atrial samples, TTR amyloid deposition was associated with disruption of the normal tissue architecture, abnormalities of myocyte morphology including attenuation and atrophy, thinning and fragmentation, vascular amyloid deposits with vessel

**TABLE 4 Multivariable Cox Regression Analysis of Risk of Death**

| | Multivariable | |
|---|---|---|
| | HR (95% CI) | *P* Value |
| IVSD | 1.00 (0.93-1.09) | 0.864 |
| RWT | 0.80 (0.29-2.19) | 0.665 |
| SV indexed | 0.98 (0.96-1.00) | 0.120 |
| LVLS (%) | 1.07 (1.03-1.12) | 0.002 |
| Significant TR | 0.98 (0.73-1.31) | 0.90 |
| Significant MR | 1.35 (1.03-1.77) | 0.032 |
| RA area indexed | 1.05 (1.01-1.10) | 0.033 |
| TAPSE/PASP | 1.73 (0.75-3.96) | 0.195 |
| T60A vs wild-type | 1.25 (0.81-1.94) | 0.314 |
| V122I vs wild-type | 1.49 (1.12-1.97) | 0.006 |
| LA area indexed | 1.01 (0.96-1.06) | 0.725 |
| ln LA stiffness | 1.23 (1.03-1.49) | 0.029 |
| Heart rate | 0.99 (0.99-1.01) | 0.827 |
| Non-SR vs SR | 1.14 (0.88-1.47) | 0.312 |
| Diagnosis before vs after February 9, 2015 | 1.52 (1.13-2.06) | 0.006 |

Abbreviations as in Table 2.

remodeling, and a decrease in the capillary network. Importantly, proteomic analysis, as well as immunohistochemistry, confirmed that amyloid was of TTR type and not atrial natriuretic peptide amyloid. These results substantiate a primary contribution of interstitial and subendocardial TTR amyloid deposits to the structural changes within the atrial wall, supporting the hypothesis of primary atrial failure associated with TTR amyloid deposition rather than a phenomenon that is predominantly secondary to LV systolic and diastolic dysfunction. This hypothesis is also supported by the results of the linear regression for LA reservoir function (Supplemental Table 2), which showed a very low ability of LV diastolic variables in the prediction of the LA mechanics.

For decades, few studies have focused on the role of atrial chambers in the pathophysiology of cardiac amyloidosis, with the vast majority of studies focusing on the degree and consequences of amyloid infiltration within the ventricles (22). Our findings suggest that atrial amyloid infiltration with associated increase in LA stiffness is an important component of overall cardiac performance, being independently associated with prognosis after adjusting for all known independent predictors, including all the deformation and nondeformation-based ventricular structural and functional parameters. Of note, atrial stiffness was an independent predictor of prognosis, whereas atrial dilatation was not in the multivariable analysis. This finding mirrors the accepted pathophysiological model associated with ventricular amyloid infiltration, in which progressive extracellular amyloid infiltration increases myocardial stiffness and results in concentric remodeling with small noncompliant chambers. Remarkably, this specific LA remodeling differs from the typical changes observed in HF with reduced EF or severe MR, in which the LA dilatation is the predominant characteristic, followed by reservoir disfunction, and stiffness increase. In ATTR-CM, the increased stiffness, and the consequent loss of distensibility, prevent atrial dilatation, making the atrial dysfunction a better marker of atrial infiltration compared with atrial dimensions.

Increased LA stiffness is associated with deterioration in the 3 atrial phasic function components: ie, progressive decline in the LA reservoir, conduit, and contraction phase (Figure 3). During ventricular systole, the atrial chamber acts as a nondistensible reservoir, increasing LA pressures and reducing the energy stored in the walls. The latter affects the conduit phase, leading to lower energy restitution to the blood flow during the ventricular diastole. LA infiltration affects the active phase in late-ventricular diastole, when the atrial contraction can be reduced or, in more severe cases, absent. Remarkably, approximately one-fifth of patients in SR showed no evidence of atrial mechanical contraction on strain analysis, despite the presence of P wave on the 12-lead electrocardiogram, a form of AEMD. The concept of AEMD has already been reported in cardiac amyloidosis (23,24); however, this is the first systematic assessment in a large population of patients with ATTR amyloidosis. Patients in SR, with and without atrial mechanical contraction, showed distinct phenotypes, with patients in SR and no mechanical contraction having a significantly worse clinical and echocardiographic phenotype compared with patients in SR whose atrial mechanical contraction was preserved. But the importance of AEMD goes beyond echocardiographic curiosity. Patients in SR with no atrial contraction have a significantly worse prognosis compared to patients in SR with mechanical contraction, likely reflecting differences in the hemodynamic contribution of LA contraction to the overall cardiac performance, to a degree comparable with patients in AF. Finally, as is the case in AF, impaired atrial contraction in SR is associated with increased risk of thromboembolization (25,26), and prophylactic anticoagulation may therefore be warranted in patients with ATTR amyloidosis in whom atrial mechanical failure is documented by atrial strain analysis.

**STUDY LIMITATIONS.** Atrial strain was analyzed retrospectively, with 26.9% of cases resulting unsuitable for the analysis. However, this is the largest cohort explored so far using this technique, providing

**CENTRAL ILLUSTRATION** **Clinical Importance of Left Atrial Infiltration in ATTR-CM**

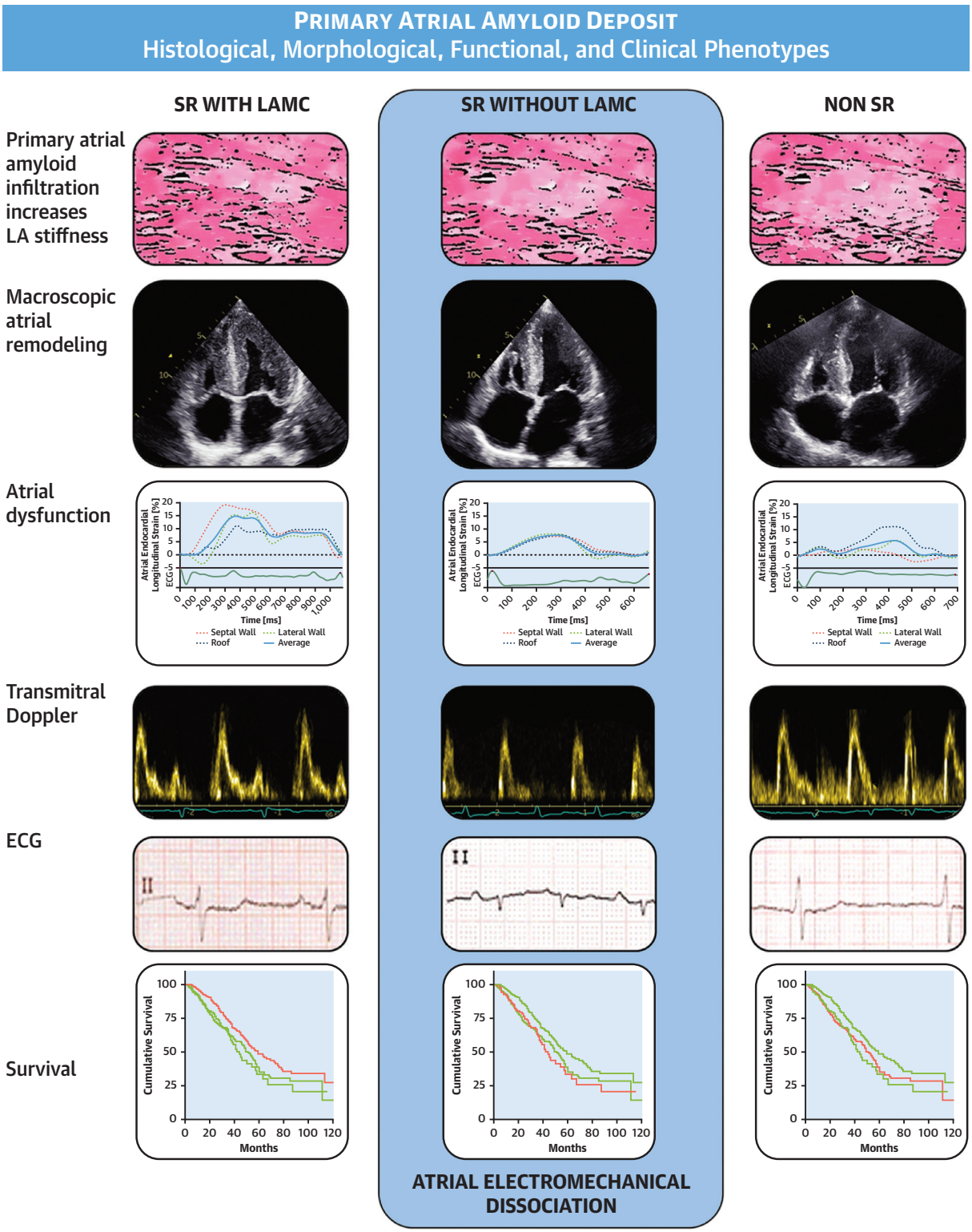


**Bandera, F. et al. J Am Coll Cardiol Img. 2022;15(1):17–29.**

Main histologic, echocardiographic, mechanical, Doppler, electrocardiographic (ECG), and survival characteristics, according to the 3 rhythm phenotypes. ATTR-CM = transthyretin amyloid cardiomyopathy; LA = left atrium; LAMC = left atrial mechanical contraction; SR = sinus rhythm.

important insight on the clinical relevance of atrial-strain measurement in cardiac ATTR amyloidosis. Strain analysis was performed using a single vendor software (Echo PAC software, GE Healthcare), and we acknowledge that intervendor variability has been reported. We do not present reproducibility in this cohort; however, intra- and interobserver reproducibility for atria strain analysis has already been published (27). We do not have echo data on the 5 explanted hearts. Data on development of AF or rate of AF ablation procedures—although the latter is likely to be very low—are not available in this population. Further studies focusing on the relationship between atrial dysfunction and occurrence of AF will be needed to explore this point. Finally, the incidence of thromboembolic events during the follow-up is not known in this population. This is a very interesting field that will need further studies.

## CONCLUSIONS

In cardiac ATTR amyloidosis, extensive amyloid deposits accumulate not only in the ventricles but also within the LA, associated with loss of normal tissue architecture and vessel remodeling. LA stiffness emerged in this study as a new independent prognostic marker, associated with reduction of reservoir, conduit, and contraction functions. The use of myocardial deformation analysis allowed the identification of AEMD, a distinct clinical phenotype associated with poor prognosis, meriting consideration of anticoagulation.

## FUNDING SUPPORT AND AUTHOR DISCLOSURES

Dr Fontana is supported by a British Heart Foundation Intermediate Clinical Research Fellowship (FS/18/21/33447). All other authors have reported that they have no relationships relevant to the contents of this paper to disclose.

**ADDRESS FOR CORRESPONDENCE:** Dr Marianna Fontana, National Amyloidosis Centre, University College London, Royal Free Campus, Rowland Hill Street, London NW3 2PF, United Kingdom. E-mail: m.fontana@ucl.ac.uk.

## PERSPECTIVES

**COMPETENCY IN MEDICAL KNOWLEDGE:** The LA involvement in ATTR-CM is not limited to chamber dilatation but implies the loss of physiological function (reservoir, conduit, and contraction) related to increased stiffness chamber.

**COMPETENCY IN PATIENT CARE AND PROCEDURAL SKILLS:** The LA strain, as assessed by echocardiography, is a reliable method to quantify the contractile function. This approach, matched with electrocardiographic (ECG) rhythm analysis, helps in identifying patients with electromechanical dissociation (loss of contraction despite P wave at ECG) at increased risk of death.

**TRANSLATIONAL OUTLOOK:** The LA infiltration occurring in ATTR-CM has impact on the wall structure, physical properties (ie, stiffness), and phasic functions of the chamber. The stages of atrial remodeling are associated with the risk of death. Further studies are needed to explore the expected link with heart failure and thromboembolic events, typically affecting ATTR-CM, and to expand the indications for thromboembolic prophylactic therapy.

## REFERENCES

**1.** Maceira AM, Joshi J, Prasad SK, et al. Cardiovascular magnetic resonance in cardiac amyloidosis. *Circulation*. 2005;111:186–193.

**2.** Fontana M, Banypersad SM, Treibel TA, et al. Native T1 mapping in transthyretin amyloidosis. *J Am Coll Cardiol Img*. 2014;7(2):157–165.

**3.** Rapezzi C, Quarta CC, Guidalotti PL, et al. Role of 99mTc-DPD scintigraphy in diagnosis and prognosis of hereditary transthyretin-related cardiac amyloidosis. *J Am Coll Cardiol Img*. 2011;4(6):659–670.

**4.** Maurer MS, Bokhari S, Damy T, et al. Expert consensus recommendations for the suspicion and diagnosis of transthyretin cardiac amyloidosis. *Circ Heart Fail*. 2019;12(9):e006075.

**5.** Gillmore JD, Maurer MS, Falk RH, et al. Nonbiopsy diagnosis of cardiac transthyretin amyloidosis. *Circulation*. 2016;133(24):2404–2412.

**6.** Lane T, Fontana M, Martinez-Naharro A, et al. Natural history, quality of life, and outcome in cardiac transthyretin amyloidosis. *Circulation*. 2019;140(1):16–26.

**7.** Chacko L, Martone R, Cappelli F, Fontana M. Cardiac amyloidosis: updates in imaging. *Curr Cardiol Rep*. 2019;21(9):108.

**8.** Fontana M, Pica S, Reant P, et al. Prognostic value of late gadolinium enhancement cardiovascular magnetic resonance in cardiac amyloidosis. *Circulation*. 2015;132(16):1570–1579.

**9.** Martinez-Naharro A, Treibel TA, Abdel-Gadir A, et al. Magnetic resonance in transthyretin cardiac amyloidosis. *J Am Coll Cardiol*. 2017;70(4):466–477.

**10.** Chacko L, Martone R, Bandera F, et al. Echocardiographic phenotype and prognosis in transthyretin cardiac amyloidosis. *Eur Heart J*. 2020;41(14):1439–1447.

**11.** Knight DS, Zumbo G, Barcella W, et al. Cardiac structural and functional consequences of amyloid deposition by cardiac magnetic resonance and echocardiography and their prognostic roles. *J Am Coll Cardiol Img*. 2019;12(5):823–833.

**12.** Bisbal F, Baranchuk A, Braunwald E, Bayés de Luna A, Bayés-Genís A. Atrial failure as a clinical entity: JACC Review Topic of the Week. *J Am Coll Cardiol*. 2020;75(2):222–232.

**13.** Thomas L, Marwick TH, Popescu BA, Donal E, Badano LP. Left atrial structure and function, and left ventricular diastolic dysfunction: JACC State-of-the-Art Review. *J Am Coll Cardiol*. 2019;73(15):1961–1977.

**14.** Kurt M, Wang J, Torre-Amione G, Nagueh SF. Left atrial function in diastolic heart failure. *Circ Cardiovasc Imaging*. 2009;2(1):10–15.

**15.** Aquaro GD, Morini S, Grigoratos C, et al. Electromechanical dissociation of left atrium in

patients with cardiac amyloidosis by magnetic resonance: prognostic and clinical correlates. *Int J Cardiol Heart Vasc*. 2020;31:100633.

**16.** Nochioka K, Quarta CC, Claggett B, et al. Left atrial structure and function in cardiac amyloidosis. *Eur Heart J Cardiovasc Imaging*. 2017;18(10):1128–1137.

**17.** Mohty D, Boulogne C, Magne J, et al. Prognostic value of left atrial function in systemic light-chain amyloidosis: a cardiac magnetic resonance study. *Eur Heart J Cardiovasc Imaging*. 2016;17(9):961–969.

**18.** Badano LP, Kolias TJ, Muraru D, et al. Standardization of left atrial, right ventricular, and right atrial deformation imaging using two-dimensional speckle tracking echocardiography: a consensus document of the EACVI/ASE/Industry Task Force to standardize deformation imaging. *Eur Heart J Cardiovasc Imaging*. 2018;19(6):591–600.

**19.** Sugimoto T, Robinet S, Dulgheru R, et al. Echocardiographic reference ranges for normal left atrial function parameters: results from the EACVI NORRE study. *Eur Heart J Cardiovasc Imaging*. 2018;19(6):630–638.

**20.** Klein AL, Hatle LK, Taliercio CP, et al. Prognostic significance of Doppler measures of diastolic function in cardiac amyloidosis: a Doppler echocardiography study. *Circulation*. 1991;83(3):808–816.

**21.** Plehn JF, Southworth J, Cornwell GGI. Brief report: atrial systolic failure in primary amyloidosis. *N Engl J Med*. 1992;327(22):1570–1572.

**22.** Martinez-Naharro A, Baksi AJ, Hawkins PN, Fontana M. Diagnostic imaging of cardiac amyloidosis. *Nat Rev Cardiol*. 2020;17(7):413–426.

**23.** Dubrey S, Pollak A, Skinner M, Falk RH. Atrial thrombi occurring during sinus rhythm in cardiac amyloidosis: evidence for atrial electromechanical dissociation. *Br Heart J*. 1995;74(5):541–544.

**24.** Stables RH, Ormerod OJ. Atrial thrombi occurring during sinus rhythm in cardiac amyloidosis: evidence for atrial electromechanical dissociation. *Heart*. 1996;75(4):426.

**25.** Leung M, van Rosendael PJ, Abou R, et al. Left atrial function to identify patients with atrial fibrillation at high risk of stroke: new insights from a large registry. *Eur Heart J*. 2017;39(16):1416–1425.

**26.** Martinez-Naharro A, Gonzalez-Lopez E, Corovic A, et al. High prevalence of intracardiac thrombi in cardiac amyloidosis. *J Am Coll Cardiol*. 2019;73(13):1733–1734.

**27.** Oxborough D, George K, Birch KM. Intra-observer reliability of two-dimensional ultrasound derived strain imaging in the assessment of the left ventricle, right ventricle, and left atrium of healthy human hearts. *Echocardiography*. 2012;29(7):793–802.

**KEY WORDS** amyloidosis, atrial function, atrial histology, atrial stiffness, atrial strain, echocardiography

**APPENDIX** For supplemental tables, please see the online version of this paper.